

# Simultaneous X-ray diffraction and calorimetric study of metastable-to-stable solid phase transformation of 1,2-dipalmitoyl-*sn*-glycerol

Hiroshi Takahashi<sup>a,\*</sup>, Motonari Watanabe<sup>a</sup>, Peter J. Quinn<sup>b</sup>,  
Ichiro Hatta<sup>a</sup>

<sup>a</sup>Department of Applied Physics, Graduate School of Engineering, Nagoya University, Nagoya 464-8603, Japan

<sup>b</sup>Division of Life Sciences, King's College London, Campden Hill, London, W8 7AH, UK

Received 9 December 1998; received in revised form 10 February 1999; accepted 10 February 1999

---

## Abstract

The thermal behaviour and structural changes associated with the phase transformation of 1,2-dipalmitoyl-*sn*-glycerol (DPG) were studied by means of simultaneous X-ray diffraction and differential scanning calorimetry. Metastable DPG solid phases are crystallized from the melted sample by thermal quenching. The metastable phase ( $\alpha$ -phase) formed initially is converted into a stable phase ( $\beta'$  phase) at  $\sim 50^\circ\text{C}$  on heating. It was found that the behaviour of the  $\alpha$ - to  $\beta'$ -phase transformation depends on the thermal history. DPG solid samples incubated at  $\sim 3^\circ\text{C}$  for more than 10 h after cooling transformed directly into the  $\beta'$ -phase with heat release. On the other hand, in the solid samples without incubation, the  $\alpha$ -phase once melted and then the crystallization of the  $\beta'$ -phase occurred successively from the melted state. © 1999 Elsevier Science B.V. All rights reserved.

**Keywords:** Diacylglycerol; Polymorphic phase behavior; DSC; X-ray diffraction; Nucleation

---

## 1. Introduction

The lipid matrix of biological membranes is said to consist of a bilayer of polar lipids of which the diacylglycerol lipids predominate in most cell membranes. The enzymatic hydrolysis of the polar

groups of these lipids can be triggered by agonists outside the cell, resulting in the accumulation of appreciable amounts of diacylglycerol (DAG) in the membrane [1]. The presence of DAG in the membrane is known to be one of the key components of transmembrane signal transduction processes [2–4], since it has been shown to modulate the activity of various membrane enzymes [5,6] and mediate fusion between lipid bilayer membranes [7,8].

---

\* Corresponding author. Tel.: +81-52-789-3709; fax: +81-52-789-3724; e-mail: takahashi@sephia.nuap.nagoya-u.ac.jp

To investigate the molecular mechanisms underlying these biochemical events, the physicochemical properties of mixtures containing DAGs and phospholipids have been widely investigated using a variety of biophysical techniques [9–20]. A knowledge of the physicochemical properties of each of the components is indispensable to a reliable interpretation of the results obtained with mixtures. Despite their biological relevance, however, there are relatively few studies of the physicochemical properties of pure DAGs compared to those of pure phospholipids.

Among the various DAGs, dipalmitoylglycerol (DPG) has been investigated in some detail [21–26]. The crystal structure of DPG with atomic resolution has already been reported [24–26]. Calorimetric and diffraction studies [21–24] have revealed that DPG forms different solid phases, depending on the crystallization conditions. When DPG crystallizes from organic solvents, it forms a stable crystal phase. This phase is denoted  $\beta'$  phase by Kodali et al. [22]. In the  $\beta'$ -phase, the hydrocarbon chains are packed in an orthorhombic subcell. Thermal quenching of melted DPG sample results in formation of a metastable crystalline phase in which the hydrocarbon chains are packed into a hexagonal subcell. This phase is designated  $\alpha$ -phase [22]. In the  $\alpha$ -phase above 26°C, the hydrocarbon chains are perpendicular to the bilayer plane, while, below 26°C, the chains become tilted [27]. A transformation from metastable  $\alpha$ -phase to stable  $\beta'$ -phase takes place on heating. Calorimetric studies have revealed that in this transformation, DPG exhibits two types of thermal events, depending on the condition of temperature treatment before the measurements, i.e. the thermal history of the sample [22,27]. In one case the phase transformation occurs with both endothermic and exothermic events around 50°C. This suggests that there are two pathways in the solid phase transformation from the  $\alpha$ -phase to the  $\beta'$ -phase, depending on the thermal history. To our knowledge, however, no direct structural evidence for the two pathways has been reported.

The aim of this study is to characterise the precise structural changes during the phase transformations of DPG and to relate the structural

changes with the thermal events. Independent measurements using differential scanning calorimetry (DSC) and X-ray diffraction were performed in addition to simultaneous X-ray diffraction and DSC measurements using a synchrotron X-ray source. The present study clearly showed that, in the case of the DPG samples incubated at  $\sim 3^\circ\text{C}$  for more than 10 h, the  $\alpha$ -phase is converted directly into the  $\beta'$ -phase but that without incubation at low temperatures, the  $\alpha$ -phase is transformed into the  $\beta'$ -phase by way of a melted phase.

## 2. Material and methods

The 1,2-dipalmitoyl-*sn*-glycerol (DPG) was purchased in powder form from Sigma Chemical Co. (St Louis, MO, USA) and used without further purification. The purity was examined by thin layer chromatography on a silica gel plate developed using solvent systems consisting of chloroform/methanol/30% aqueous ammonia = 10:10:3 (by vol). A single spot was shown on the plate. The powder of DPG was dissolved in hexane. The solvent was evaporated under a stream of oxygen-free dry nitrogen and then, the sample was stored for  $\sim 16$  h in vacuo to remove remaining traces of solvent.

Simultaneous X-ray diffraction and DSC measurements were performed on beam line 15A of the Photon Factory at Tsukuba, Japan [29]. With the use of a modified differential scanning calorimeter (FP84, Mettler Instrument Corp., Hightstown, NJ), time-resolved X-ray diffraction and thermal data were obtained simultaneously from the same sample. The detailed method and modification of the calorimeter have been reported elsewhere [30,31]. The wavelength of the synchrotron X-rays was 0.1506 nm. The patterns of diffracted X-rays were recorded using a position sensitive proportional counter (PSPC) with 512 channels. Sample-to-detector distances were  $\sim 280$  mm and  $\sim 1500$  mm for wide- and small-angle measurements, respectively. The diffraction spacings were calibrated using the lamellar spacing of anhydrous cholesterol [32]. The powder samples ( $\sim 10$  mg) were sealed between thin aluminium foils (thickness  $\sim 40$   $\mu\text{m}$ ). All experi-

ments were performed in heating mode with a scan rate of  $1.0^{\circ}\text{C}/\text{min}$ .

DSC experiments were carried out using a DSC10/SSC580 calorimeter (Seiko I & E, Tokyo, Japan). DSC data for both heating and cooling scans were recorded at a scan rate of  $1.0^{\circ}\text{C}/\text{min}$ . Samples ( $\sim 1.5$  mg) were placed in small aluminium pans (Mettler Instrument Corp., Hightstown, NJ) and hermetically sealed.

Static X-ray diffraction measurements were carried out using a Ni-filtered  $\text{CuK}_{\alpha}$  radiation source (RU200BEH, Rigaku, Tokyo, Japan) and a two-dimensional area detector (Imaging plate, Fuji Photo Film Co. Ltd., Tokyo, Japan). The X-ray beam was focused by a double-mirror optical system. Samples sealed in glass capillary tubes were fixed to a brass hollow holder. Temperature of the sample was controlled by circulating water from a temperature-controlled water bath (B. Braun, Melsungen, Germany) through the sample mount. The data sampling of the imaging plates was performed with a BAS2000 data reading system (Fuji Photo Film Co. Ltd.).

### 3. Results

The effects of thermal history were examined with respect to the thermal behaviour of DPG, using DSC. On heating, the melting transition of DPG crystallized from hexane was observed at  $68.7^{\circ}\text{C}$  (Fig. 1a). The enthalpy was  $112$  kJ/mol. Recrystallization on cooling from isotropic melted state exhibited considerable hysteresis and the exothermic peak was observed at  $48.9^{\circ}\text{C}$  (Fig. 1b) some  $20^{\circ}\text{C}$  lower than the melting endotherm. The enthalpy of the recrystallization ( $60$  kJ/mol) was less than that of the melting transition observed for the initial heating scan, because the initial solid phase formed by cooling from the melted state is a metastable  $\alpha$ -phase [21–23]. This was confirmed by static X-ray diffraction (Fig. 2). The X-ray diffraction pattern of the  $\beta'$ -phase (Fig. 2a) is characterised by multiple wide-angle diffraction peaks compared with the  $\alpha$ -phase where the wide-angle scattering region is dominated by a single symmetrical peak at a spacing of  $0.413$  nm (Fig. 2b). This indicates that the metastable phase is more disordered than the

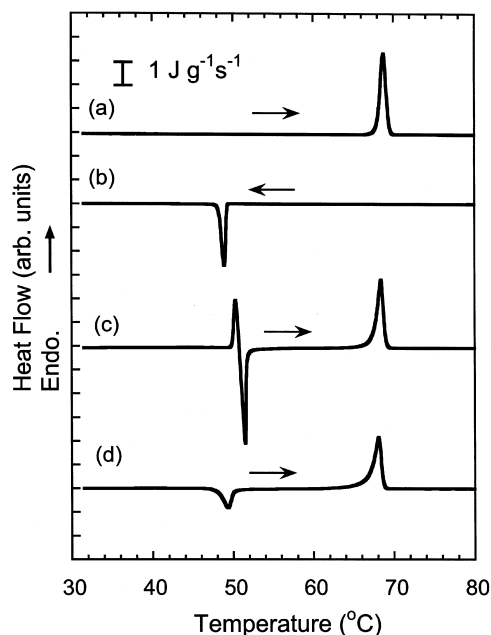


Fig. 1. DSC thermograms of the DPG samples. (a) Initial heating thermogram of DPG crystallized from hexane. (b) Cooling thermogram from the DPG melt. (c) Second heating thermogram obtained from the sample without incubation after cooling. (d) Second heating thermogram obtained from the sample incubated at  $\sim 3^{\circ}\text{C}$  for 10 h. All scan rates were  $1.0^{\circ}\text{C}/\text{min}$ .

stable phase. These DSC results of the first heating and cooling scans agree with previous calorimetric studies [22,23].

The second heating DSC curves were different from the first heating scan for crystallized samples from organic solvents and showed the dependence on the thermal history of the samples (Fig. 1c,d). The immediate second heating scan showed three separate peaks in the thermogram (Fig. 1c); an endothermic peak at  $50.3^{\circ}\text{C}$  followed closely by an exothermic peak at  $51.6^{\circ}\text{C}$  and a higher temperature endothermic transition with the enthalpy of  $112$  kJ/mol at  $68.3^{\circ}\text{C}$ . The enthalpies of the transitions around  $50^{\circ}\text{C}$  are difficult to calculate accurately but the enthalpy of the exothermic transition was invariably greater than that of the endothermic transition. Hence, the net heat flow of the transitions around  $50^{\circ}\text{C}$  was exothermic and the overall enthalpy is  $\sim 40$  kJ/mol. Judging from the temperature and the enthalpy of the

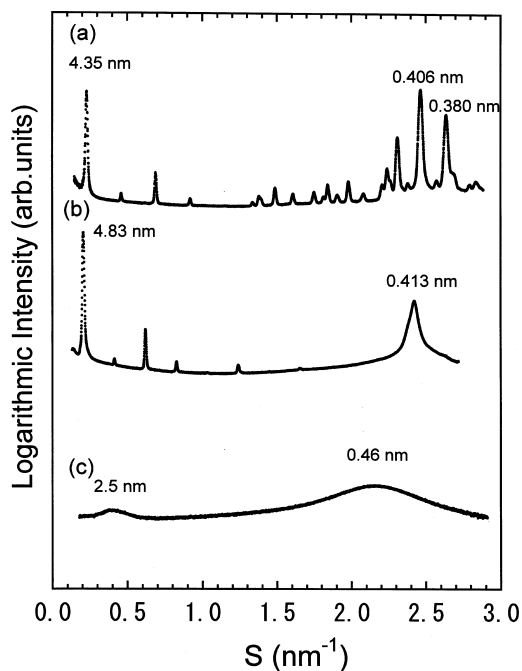


Fig. 2. Static X-ray diffraction patterns of DPG recorded from (a) a hexane-crystallized sample at 20°C ( $\beta'$ -phase). (b) A crystallized sample at 20°C ( $\alpha$ -phase) formed immediately on cooling from the melt. (c) The malt at 75°C. ( $S = 2\sin\theta/\lambda$ ;  $2\theta$  = scattering angle,  $\lambda$  = wavelength of X-rays).

higher temperature endothermic transition, the endothermic and exothermic events in the temperature region of 50°C can be interpreted as a melting transition from the  $\alpha$ -phase and subsequent recrystallization to the  $\beta'$ -phase [22,23]. Direct evidence supporting this interpretation was obtained from simultaneous X-ray diffraction and DSC measurements as described below. As Shannon et al. have pointed out [23], the broadness of the melting transition of the  $\beta'$ -phase (Fig. 1c) relative to solvent-crystallized sample (Fig. 1a) may represent a degree of crystal imperfection with the  $\beta'$ -form recrystallized after the melting transition of the  $\alpha$ -phase.

An indication of the rate of relaxation of the metastable phase into the stable crystalline phase was examined by studying the effect of incubation time on the thermal events around ~50°C. Samples stored for longer than 10 h at ~3°C after cooling from the melted state showed two transition enthalpies in heating thermograms. For the

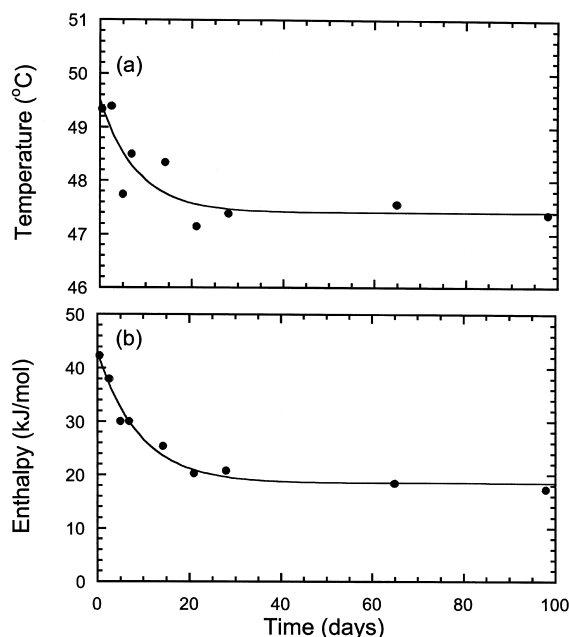


Fig. 3. Plots of (a) the transition temperature and (b) the enthalpy of the exothermic transition of DPG incubated at ~3°C as a function of the incubation time.

sample incubated at ~3°C for 10 h, an exothermic peak was observed at ~49°C and an endothermic peak at 69°C (Fig. 1d). This thermogram (Fig. 1d) is almost the same to that obtained from DPG samples incubated 40 days at 15°C [28]. The peak temperature and enthalpy of the exothermic peak around ~49°C decreased exponentially with incubation time up to 30 days (Fig. 3) whereupon it reached a constant value. The peak temperature and enthalpy of the endothermic transition observed at ~69°C is consistent with a melting transition of the  $\beta'$ -phase. The decrease of the enthalpy with increasing incubation times clearly suggests that the domain of the  $\beta'$ -phase grows in the  $\alpha$ -phase by incubating at ~3°C. This was confirmed by X-ray diffraction measurements. In addition to the small-angle diffraction peak assigning to the  $\alpha$ -phase, a weak diffraction peak was observed in the small-angle X-ray diffraction pattern recorded at 20°C in the sample incubated at ~3°C for 400 h after cooling from the melted state (Fig. 4). The spacing of this minor peak is consistent with a coexisting the

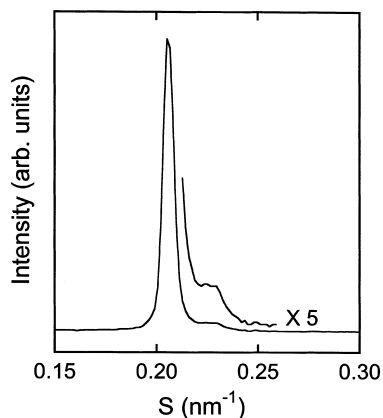


Fig. 4. Small-angle X-ray diffraction pattern from a sample of DPG incubated at  $\sim 3^{\circ}\text{C}$  for 400 h recorded at  $20^{\circ}\text{C}$ . The patterns are also shown in a fivefold expanded vertical scale in the range of  $0.21 < S < 0.26 \text{ nm}^{-1}$ .

domain of  $\beta'$ -phase formed from  $\alpha$ -phase during incubation at  $3^{\circ}\text{C}$ .

To characterise the structural changes that take place in the temperature region of  $50^{\circ}\text{C}$  in the temperature scans of samples reheated immediately after cooling or after incubation at  $\sim 3^{\circ}\text{C}$ ,

we carried out simultaneous X-ray diffraction and DSC measurements. In order to get high resolution data, scattering from of small- and wide-angles were acquired separately using different camera lengths. It is conceivable that small differences could occur in the thermal history of samples prepared for the two measurements but because simultaneous thermal and diffraction data were collected from each the comparison between thermal events and structural changes is valid. Figure 5 presents small-angle X-ray diffraction patterns recorded from the simultaneous measurements. Within the resolution in these experiments, only two Bragg diffraction peaks at 4.82 nm and 4.37 nm were observed. Judging from these spacings and the wide-angle diffraction data (Fig. 7), we tentatively assign the diffraction peak at 4.82 nm to the  $\alpha$ -phase of DPG and that the peak at 4.37 nm to the  $\beta'$ -phase. No other intermediate ordered phase formed during the transformation from the  $\alpha$ -phase to the  $\beta'$ -phase could be detected from the X-ray data. The diffraction peaks of the  $\beta'$ -phase appeared only after com-

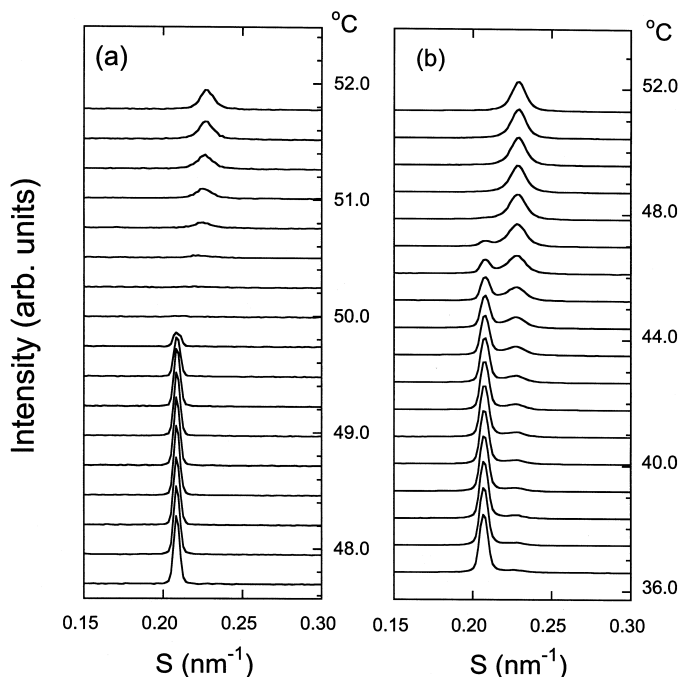


Fig. 5. Small-angle diffraction patterns recorded using simultaneous X-ray diffraction and DSC methods with a heating scan rate of  $1.0^{\circ}\text{C}/\text{min}$ . (a) DPG without incubation after cooling from the melted state. (b) DPG after incubation at  $\sim 3^{\circ}\text{C}$  for 400 h.

plete disappearance of that of the  $\alpha$ -phase in the sample without incubation (Fig. 5a). By contrast, a coexistence of  $\alpha$ - and  $\beta'$ -phases was observed during the transformation in the sample incubated at  $\sim 3^\circ\text{C}$  for 400 h (Fig. 5b). As described above, this coexistence was detected at even  $20^\circ\text{C}$  (Fig. 4). The decrease intensities of the  $\alpha$ -phase diffraction peak was associated with corresponding increase of intensity of the  $\beta'$ -phase with increasing temperature.

To clarify the relationship between the thermal events and structural changes during the metastable-to-stable phase transformation, the change of intensity in X-ray scattering in the small-angle diffraction region and simultaneous DSC data are plotted in the same graphs (Fig. 6). It can be seen from these data that the onset and completion of the thermal events are highly correlated with those of change in the diffraction intensity. In the DPG sample reheating immediately, the temperature of the endothermic peak coincides with the temperature at which no distinct X-ray diffraction peak was observed in the small-angle X-ray scattering region (Fig. 6a).

Wide-angle measurements were also performed on the samples with or without the incubation at  $\sim 3^\circ\text{C}$  for 40 h (Figs. 7 and 8). Both wide-angle diffraction patterns of samples with or without incubation at  $3^\circ\text{C}$  in the temperature range below  $\sim 49^\circ\text{C}$  were characterized by a single symmetric peak centred  $2.4\text{ nm}^{-1}$  ( $d = 4.2\text{ nm}$ ) (Fig. 7a and Fig. 8a). This indicates that the hydrocarbon chains are packed into a hexagonal lattice ( $\alpha$ -phase). The width of the diffraction peaks differs between samples shown in Fig. 7a and Fig. 8a, because slits with different widths were placed in the front of the detector. In the sample reheated immediately without incubation, the intensities of the wide-angle diffraction peak of the  $\alpha$ -phase decreased abruptly as the temperature approached  $49^\circ\text{C}$  and at  $50.3^\circ\text{C}$  only a broad diffraction band was observed (Fig. 7a). The diffuse Bragg scattering in the wide-angle region indicates that the hydrocarbon chains become disordered as the  $\alpha$ -phase melts. Upon heating above  $\sim 50^\circ\text{C}$ , three diffraction peaks appear which are centred at  $2.25\text{ nm}^{-1}$  ( $d = 0.44\text{ nm}$ ),  $2.45\text{ nm}^{-1}$  ( $d = 0.41\text{ nm}$ ), and  $2.6\text{ nm}^{-1}$  ( $d = 0.38$

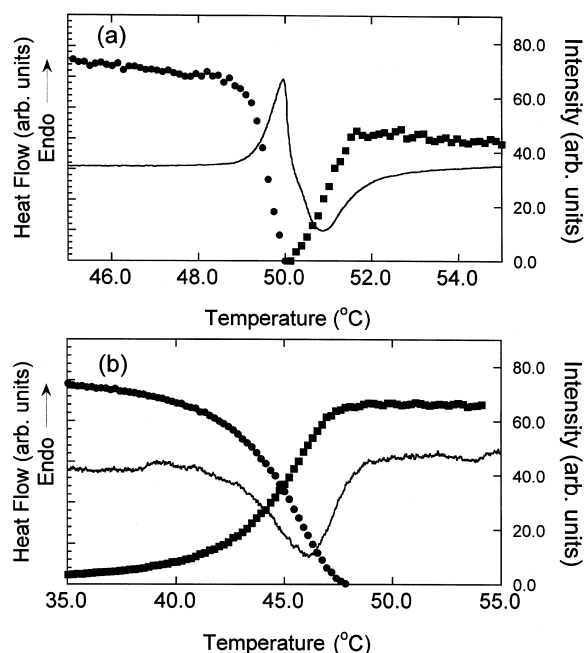


Fig. 6. Comparison between the small-angle X-ray diffraction and DSC data obtained from the simultaneous measurements. (a) DPG reheated immediately without incubation after cooling from the melted state. (b) DPG after incubation at  $\sim 3^\circ\text{C}$  for 400 h; (—) DSC data; (●) intensities of the diffraction peak of the  $\alpha$ -phase; (■) intensities of the diffraction peak of the  $\beta'$ -phase.

nm). This diffraction pattern is similar to that of DPG crystallized from organic solvent (Fig. 2a). This data indicates that the  $\beta'$ -phase was crystallized from a melted phase of DPG. The structural transitions observed by diffraction measurements coincide precisely with the thermal data recorded simultaneously. The temperature at which only a broad diffraction peak was observed corresponds to the temperature of the endothermic DSC peak (Fig. 7). This result is in good agreement with that obtained from the small-angle experiments (see Fig. 6a). The effect of storage of the DPG at  $\sim 3^\circ\text{C}$  for 40 h after cooling from the melted state is illustrated in Fig. 8. This shows evidence for a coexistence of the diffraction peaks characterizing the  $\alpha$ - and  $\beta'$ -phases, respectively, with no apparent disordering of the hydrocarbon chains over the temperature range in which the exothermic peak appeared in the DSC curve (Fig. 8). This result implies that the DPG incubated at

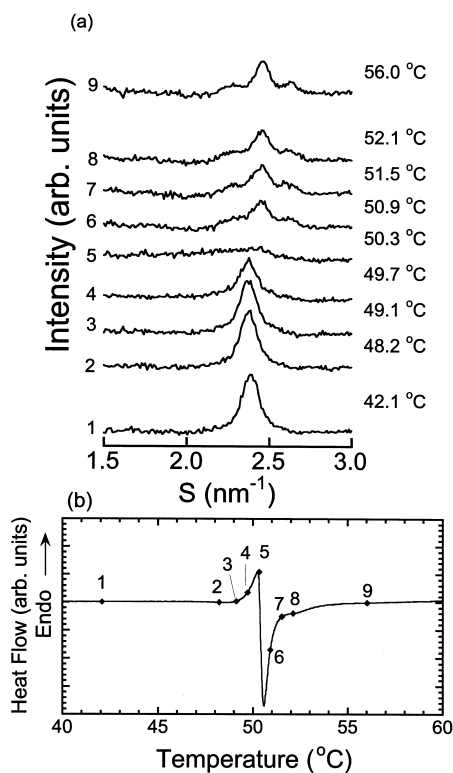


Fig. 7. (a) Wide-angle X-ray diffraction patterns for DPG reheated immediately without incubation after cooling from the melt using simultaneous X-ray diffraction and DSC methods with a heating scan of  $1.0^{\circ}\text{C}/\text{min}$ . The temperature at which each pattern was recorded is indicated on the right side of each pattern. The numbers on the left side refer to the numbers on the DSC thermograms. (b) The corresponding DSC thermograms.

a low temperature undergoes a two-state transition in which the  $\alpha$ -phase transforms directly into the  $\beta'$ -phase with no detectable intermediate phase.

#### 4. Discussion

The present results clearly distinguish between two pathways in transformation of DPG from the  $\alpha$ - to  $\beta'$ -phase, depending on the thermal history. The DPG in the  $\alpha$ -phase without prolonged incubation at low temperature transforms into the  $\beta'$ -phase by way of a disordered melted phase as indicated from direct observation of structural changes at the molecular level. On the other

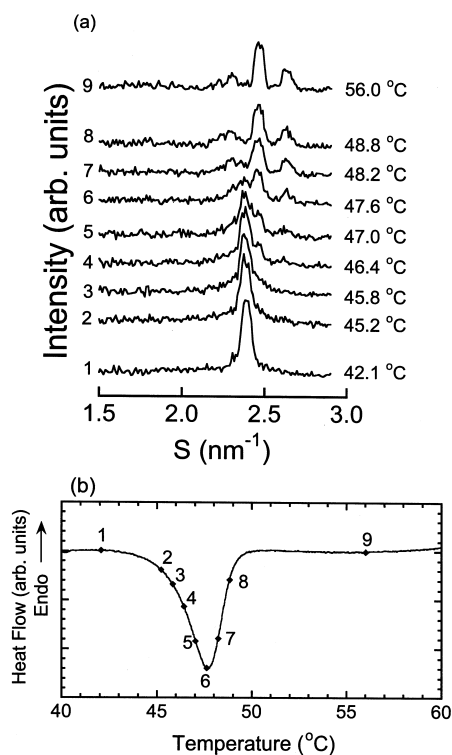


Fig. 8. (a) Wide-angle X-ray diffraction patterns for DPG incubated at  $\sim 3^{\circ}\text{C}$  for 40 h after cooling from the melt using simultaneous X-ray diffraction and DSC methods with a heating scan of  $1.0^{\circ}\text{C}/\text{min}$ . The temperature at which each pattern was recorded is indicated on the right side of each pattern. The numbers on the left side refer to the numbers on the DSC thermograms. (b) The corresponding DSC thermograms.

hand, when DPG is incubated at  $\sim 3^{\circ}\text{C}$  for more than 10 h, the  $\alpha$ -phase appears to be converted directly into the  $\beta'$ -phase.

On the basis of previous results obtained by calorimetry, Kodali et al. [22] and Albon and co-workers [27,28] have concluded that the process of phase transformation from the  $\alpha$ -phase to  $\beta'$ -phase of DPG is consistent with a nucleation and growth process. Let us consider the present results for the  $\alpha$ - to  $\beta'$ -phase transformation from the viewpoint of the growth of the  $\beta'$ -phase domain. Similar discussions have been published for solid-state transformation of triacylglycerols [33,34].

In the case without prolonged incubation at low temperature, it is expected that the growth

rate of the  $\beta'$ -phase in the  $\alpha$ -phase will be slower than that in the melted state, due to the slow mobility of molecules and the relatively high density of the  $\alpha$ -phase in comparison with the melted phase. Hence, the domain of the  $\beta'$ -phase formed immediately on cooling from the melt cannot grow rapidly in the  $\alpha$ -phase during heating compared with the melted phase. In contrast, after melting of the  $\alpha$ -phase, a rapid growth of the  $\beta'$ -phase occurs in the melted phase. The growth rate of the  $\beta'$ -phase is slow in the  $\alpha$ -phase, but a prolonged incubation at low temperature allows the formation of the relatively large domain of the  $\beta'$ -phase which can be detected by X-ray diffraction. Generally a larger domain has a smaller ratio of an interfacial surface area to volume than a small domain. Thus, it can be inferred that, as domains become bigger, the inhibitory effect of the interfacial energy between stable and metastable phases on the domain growth progressively diminished and the domain growth can accelerate. As a result, direct transformation from the  $\alpha$ -phase to the  $\beta'$ -phase occurs above  $\sim 46^\circ\text{C}$  in the sample subjected to prolonged incubation at  $3^\circ\text{C}$ .

The results presented in this work demonstrate clearly that the phase behaviour of DPG depends markedly on the thermal history of the sample. We may therefore anticipate that the phase behaviour of binary mixtures of phospholipids and DPG may also depend on the thermal history. Some support for this idea has been obtained from studies of mixtures of 1,2-dipalmitoylphosphatidylcholine and DPG in which mixtures where DPG exceed 60 mol% a metastable behaviour of phase separated DPG was observed but there was no detectable hysteresis in the thermal behaviour of the complex formed by the two lipids [17].

### Acknowledgements

Part of this work has been performed under approval of the Photon Factory Program Advisory Committee (Proposal No. 96G068). A BAS2000 system was used with consent of the High Intensity X-ray Diffraction Laboratory Execution Committee of Nagoya University. We are grateful

to Prof. Y. Amemiya for help of setting up the instrumentation for the synchrotron X-ray diffraction experiments and also to Mr T. Hikage for technical support of the BAS2000 system. This work is supported in part by Grant-in-Aid from Ministry of Education, Science, Sports and Culture, Japan and a cooperative research project award from the British Council.

### References

- [1] J. Preiss, C.R. Loomis, W.R. Bishop, R. Stein, J.E. Nidel, R.M. Bell, *J. Biol. Chem.* 261 (1986) 8597.
- [2] Y. Nishizuka, *Science* 258 (1992) 607.
- [3] M. Liscovitch, L.C. Cantly, *Cell* 77 (1994) 329.
- [4] N. Divecha, R.F. Irvine, *Cell* 80 (1995) 269.
- [5] R.M.C. Dawson, N.L. Hemington, R.F. Irvine, *Biochem. Biophys. Res. Commun.* 117 (1983) 196.
- [6] R.M.C. Dawson, R.F. Irvine, J. Bray, P.J. Quinn, *Biochem. Biophys. Res. Commun.* 125 (1984) 836.
- [7] D.P. Siegel, J. Banschach, D. Alford, et al., *Biochemistry* 28 (1989) 3703.
- [8] J. Nieva, A. Alonso, G. Basanez, et al., *FEBS Lett.* 368 (1995) 14.
- [9] T. Heimburg, U. Wurz, D. Marsh, *Biophys. J.* 63 (1992) 1369.
- [10] F. Lopez-Garcia, J. Villalain, J.C. Gomez-Fernandez, P.J. Quinn, *Biophys. J.* 66 (1994) 1991.
- [11] R.M. Epand, *Biochemistry* 24 (1985) 7092.
- [12] S. Das, R.P. Rand, *Biochemistry* 25 (1986) 2882.
- [13] A. Ortiz, J. Villalain, J.C. Gomez-Fernandez, *Biochemistry* 27 (1988) 9030.
- [14] B.A. Cunnigham, T. Tsujita, H.L. Brockman, *Biochemistry* 28 (1989) 32.
- [15] J.A. Hamilton, S.P. Bhamidiapti, D.R. Kodali, D.M. Small, *J. Biol. Chem.* 66 (1991) 1177.
- [16] H. De Boeck, R. Zidovetzki, *Biochemistry* 31 (1992) 623.
- [17] F. Lopez-Gracia, J. Villalain, J.C. Gomez-Fernandez, *Biochim. Biophys. Acta* 1190 (1994) 264.
- [18] P.J. Quinn, H. Takahashi, I. Hatta, *Biophys. J.* 68 (1995) 1374.
- [19] H. Takahashi, I. Hatta, P.J. Quinn, *Biophys. J.* 70 (1996) 1407.
- [20] A.R. Dibble, A.K. Hinderliter, J.J. Sando, R.L. Biltonen, *Biophys. J.* 71 (1996) 1877.
- [21] D.L. Dorset, *Chem. Phys. Lipids* 43 (1987) 179.
- [22] D.R. Kodali, D.A. Fahey, D.M. Small, *Biochemistry* 29 (1990) 10771.
- [23] R.J. Shannon, J. Fenerty, R.J. Hamilton, F.B. Padley, *J. Sci. Food Agric.* 60 (1992) 405.
- [24] D.L. Dorset, W.A. Pangborn, *Chem. Phys. Lipids* 48 (1988) 19.
- [25] F. Mo, B.C. Hauback, N. Albon, *J. Phys. Chem.* 97 (1993) 6083.



- [26] G. Won Han, J.R. Ruble, B.M. Craven, *Chem. Phys. Lipids* 71 (1994) 219.
- [27] A.F. Craievich, A.M. Levelut, M. Lambert, N. Albon, *J. Physique* 39 (1978) 377.
- [28] N. Albon, A.F. Craievich, *J. Phys. Chem.* 90 (1986) 3434.
- [29] Y. Amemiya, K. Wakabayashi, T. Hamanaka, T. Wakabayashi, T. Matsushita, H. Hashizume, *Nucl. Instrum. Methods* 208 (1983) 471.
- [30] I. Hatta, H. Takahashi, S. Matuoka, Y. Amemiya, *Thermochim. Acta* 253 (1995) 149.
- [31] H. Takahashi, S. Matuoka, Y. Amemiya, I. Hatta, *Chem. Phys. Lipids* 76 (1995) 115.
- [32] C.R. Loomis, G.G. Shipley, D.M. Small, *J. Lipid Res.* 20 (1979) 525.
- [33] K. Sato, *J. Phys D: Appl. Phys.* 26 (1993) B77.
- [34] S. Ueno, A. Minato, H. Seto, Y. Amemiya, K. Sato, *J. Phys. Chem. B* 101 (1997) 6847.